IS-PORTO 2023 PROCEEDINGS

Proceedings of the 8th International Symposium on
DEFORMATION CHARACTERISTICS OF GEOMATERIALS
Porto, 3rd - 6th September 2023

Effect of fibre orientation on the mechanical response of reinforced sand, detected with x-ray tomography

Michela Arciero[1#], *Erminio* Salvatore[1#], *Alessandro* Tengattini[2#], *Giuseppe* Modoni[1#] *and Gioacchino* Viggiani[2#]

[1]*University of Cassino and Southern Lazio, Department of Civil & Mechanical Engineering, via G. Di Biasio 43, 03043 Cassino, Italy*
[2] *Univ. Grenoble Alpes, Laboratoire 3SR, 1270 Rue de la Piscine, 38610 Gières, France*

[#]*Corresponding author: michela.arciero@studentmail.unicas.it*

ABSTRACT

The mechanical behaviour of fibre-reinforced sands (FRS) has been thoroughly explored with a laboratory study, firstly investigating the influence of relevant parameters such as grading index, soil density, amount, diameter, and length of fibres then focusing on their orientation with respect to the principal stress directions. This aspect has been deeply investigated performing parallel tests on samples of pure sand and on samples with randomly and uniformly oriented fibres compacted at a similarly high relative density (Dr≈1). Direct and triaxial shear tests have been performed, the former enforcing deformation on a predetermined shear plane. The results show that reinforcement with oriented fibres provides a higher strength and ductility to the sand. The grain scale investigation of the materials' response to direct shearing has been carried out performing X-ray tomography post-mortem (i.e., after the test). The evolution of porosity in several samples prepared with the same procedure and sheared under the same conditions has been studied freezing the material fabric with nanosilica grout injected at different displacement levels. On the contrary, X-ray tomography performed along with miniature triaxial tests (operando method) enabled the analysis of the spatial distribution of deviatoric strain too. In both cases, maps show the relevant role of fibres orientation with reference to the shear band. If adequately activated, fibres tension modifies the strain field in the samples, preventing the fragile rupture along a shear plane and transferring the stresses to the outer soil portions, in this way providing a more dilatant and ductile overall response of the reinforced material.

Keywords: Fibre reinforced sands; strain localization; X-ray tomography; porosity; dilatancy.

1. Introduction

The reinforcement of sands by a diffuse inclusion of fibres is object of several past studies, promoted by the idea that filaments of controlled mechanical characteristics intruded in the soil pores somehow inhibit the mobility of grains, provide additional properties to the assembly (e.g., resistance, stiffness, ductility or damping) and improve the performance of geotechnical structures (Gray, et al. (1983), Maher, et al. (1994), Park, et al. (2005), Yetimoglu, et al. (2005), Ahmad, et al. (2010)). So far, studies have mostly been conducted at the element scale with two main goals. In one case, the response of natural and differently reinforced materials to various laboratory tests has been observed to investigate the role of paramount characteristics, like soil type and density, diameter, length, concentration and tensile strength of the fibres, and optimise ground improvement (Al-Refeai, (1991), Consoli, et al. (2009), Tang, et al. (2007)). In other cases, laboratory experiments have focused on the modification of the stress-strain response to develop realistic constitutive models (e.g., Diambra, et al (2015), Gao, et al. (2020)).

In both cases, laboratory tests focus on the overall mechanical response of the reinforced material subjected to different stress conditions, and interpretation is carried out phenomenologically, i.e., comparing the stress-strain response for different testing conditions (see for instance Michalowski and Cermak, 2002; Consoli et al., 2007; Diambra, 2010, Lirer et al., 2011). The X-ray tomography technique coupled with powerful image analysis algorithms (Alshibli, et al. (2006), Matsushima, et al. (2006), Alikarami, et al. (2015), Andò, et al. (2020)) enables to investigate phenomena occurring at the particle scale, observing, characterising and quantifying local interactive mechanisms that dictate, with their spatial distribution, the overall soil response. So far, the application of the tomographic technique to fibre reinforced sands is limited (e.g., Diambra and Ibrahim, 2015; Soriano et al., 2017). A root investigation of the soil-fibres interaction upon shearing would disclose the mechanisms that take place locally and affect the global behaviour of the soil assembly, providing great benefits for the reinforcement's design and for the performance prediction.

The present study merges the two approaches, the classical one carried out at the single element scale with the microscale tomographic observation, to identify the role of fibres on the mechanical response of the

reinforced sands. Particularly importance is herein given to the effect of fibres orientation with reference to the localised strains that normally develop in sheared sand (Salvatore et al. (2019)). Bearing this goal in mind, two types of tests have been carried out, direct and triaxial shear, to see the effects of fibres when strain localization is forced along a predetermined plane or when it develops spontaneously as a function of material behaviour. Both tests have been performed on samples of Hostun sand, some of them without reinforcement, others adding randomly oriented fluorocarbon fibres, others orienting fibres near the minimum principal stress direction.

The X-ray was performed at Laboratoire 3SR in Grenoble (France). Here, the equipment allowed to perform triaxial tests on miniature samples directly in the tomograph (operando method) and the fibres placement was relatively easy. On the contrary, the analysis of samples subjected to direct shear required an ad-hoc experimental procedure described in the paper. Tests were performed with a conventional equipment out of the tomograph and samples with oriented fibres were formed with a specific method designed at the geotechnical laboratory (LAGGS) of the University of Cassino (Italy). The evolution of the microscopic characteristics upon direct shear has been detected performing parallel tests on several samples prepared with the same procedures, freezing soil fabric with nanosilica grout injections at different stages of the test and bringing samples in the tomograph (post-mortem technique).

2. Experimental setup

2.1 X-ray CT

Computed tomography (CT) is a non-destructive measurement technique that enables a quantitative description of the internal structures of bulky objects, determined by the variation of density of the scanned materials. The technique implies the acquisition of multiple radiographies of the object from different angular position around a central axis. Acquisition is followed by an image reconstruction process that provides a 3D image of the object. In the present case, the sample was rotated while the X-ray source and detector were kept in a fixed position. Each X-ray radiography of the sample is obtained averaging five scans recorded on a flat panel detector with an exposure time of 0.5 s. Axial tomography is built with 1700 radiographies over 360°. For composite materials it is essential to know the absorption versus X-ray intensity of each component, to assign the optimal power achieving maximum contrast among phases. In the present experiments, voltage and intensity equal to respectively 75kV and 120µA for the miniature triaxial test samples, and 120kV and 200µA for the direct shear test samples have been emitted from a tungsten target X-ray source, generating a divergent polychromatic X-ray beam. With this setup, pixel sizes of 15µm/px for the miniature triaxial test and 20µm/px for the direct shear test samples have been obtained.

In the miniature triaxial tests, soil grains, fibres and voids had to be distinguished, which was relatively easy considering their largely different densities (the unit weight is equal to 26.5 kN/m^3 for sand grains, and 15.2 kN/m^3 for the fluorocarbon fibres).

The greyscale images coming from X-ray tomography need to be processed in order to unequivocally assign each pixel to grain, fibre or pore phases, obtaining a trinarised image. In Fig. 1a the histogram reporting the distribution of grey-values is shown; the following thresholds are applied to detect the different sample materials: 28,700-41,100 to select fibres (and unfortunately also some pixels of grain/pore edges), all grey values less than the lower limit, belong to voids, all grey values above the upper limit, identify grains. Fibers identification, thanks to the cleanliness of tomographic images, is relatively easy.

These selected fibre pixels are reduced by one cycle of a morphological erosion, and the remaining unwanted pixels identified as connected 3D objects smaller than 1 voxel in volume are removed from the picture. The fibre map is now dilated to recover the initial volume and to finish filling any voids that may be present in the fibre map. Again, with the objective of keeping the correct fibre volume, a final erode step is applied to obtain a final fibre map. The final trinarised image results from the superposition of the thresholded grain phase to the fibre map.

On the contrary, particular care have to be placed for the scan of samples obtained from the direct shear tests. In this second case, soil pores were filled with the nanosilica grout used to freeze the material's fabric, whose density is equal to 10.8 kN/m^3, i.e. quite similar to that of fibres, made the identification of fibres more problematic (Fig. 1b). Due to the close similarity of fiber and nanosilica densities, these two phases were linked together. Although this problem does not allow a clean fibre skeleton extraction, it does not invalidate the direct shear test tomography post-processing analysis, as the fibers are considered as part of the voids. Therefore, to compute the porosity maps illustrated below, only one threshold is needed to separate the grains from its surroundings.

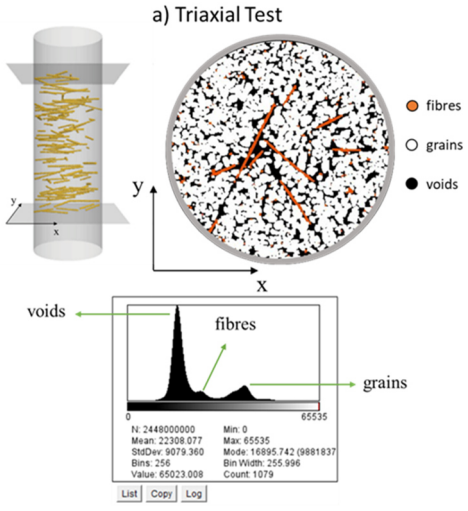

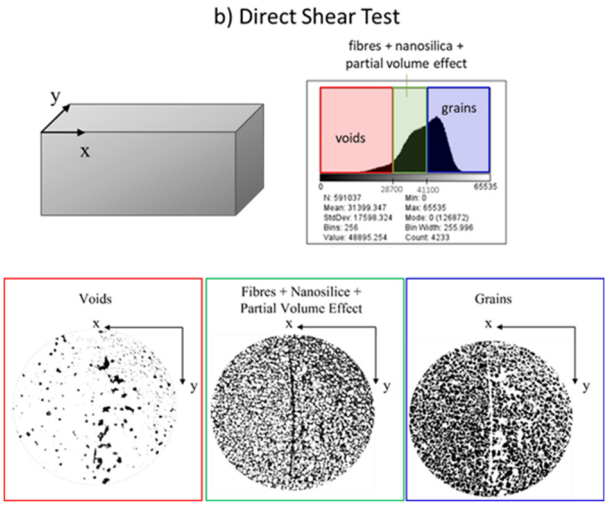

Figure 1. Histograms with distribution of grey values, corresponding to the different component phases of the material during triaxial test (a), 3 phases: grains, fibres, air, and direct shear test (b), 4 phases: grains, fibres, air, nanosilica.

3. Materials

3.1 Sand

All tests were performed on Hostun HN31, a standard material for laboratory testing. This sand consists of angular to sub-angular grains and has a silica content SiO2 > 98%. The grain size distribution is shown in Fig. 2 and its physical properties are as follows: mean grain size D_{50} = 0.32 mm, uniformity coefficient Cu = D_{60}/D_{10}=1.62, gradation coefficient Cg= $(D_{30})2/(D_{60}\cdot D_{10})$ =1.0, specific gravity Gs=2.65, minimum and maximum void ratios e_{min}=0.648 and e_{max}=1.041.

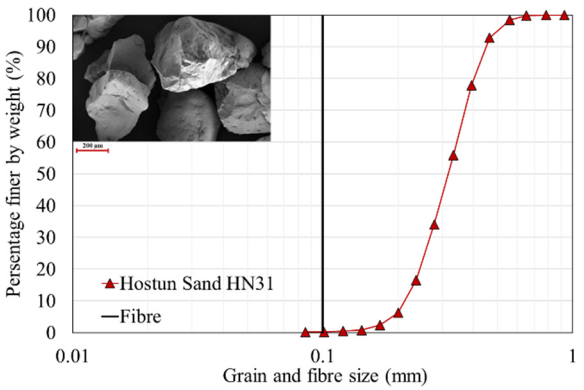

Figure 2. Grain size distribution for Hostun HN31 sand and fibre diameter.

3.2 Fibres

The most typical fibres used to reinforce soil are Polypropylene, Polyester, or PVC fibres (Ibrahim et al., 2012, Gray and Ohashi, 1983). In this work, a different type of plastic was chosen to more clearly distinguish fibres in the tomographic images. The used fibres belong to the fluorocarbon fibre group, being extracted from a fluorocarbon continuous wire used for fishing.

The parameter governing the choice of fibres is density ρ, that rules attenuation and should be markedly different from that of air and of sand in the sample to facilitate identification. In the current project, the chosen fluorocarbon fibres have a density of 15.2 kN/m^3, which is largely different and thus creates a noticeable contrast with air (around 0,01225 kN/m^3) and sand (26.5 kN/m^3).

The complete list of fibres properties, including diameter and length used for the direct and miniature triaxial tests is given in Table 1.

Table 1. Physical properties of fibres.

Dimension		Size in pixels*
Fibre length, l_f (mm)	10, 30 (DS) 10 (TX)	500, 1500 666
Fibre diameter, d_f (mm)	0.10	5 6.6
Fibre density (kN/m^3)	15.2	-
Breaking load (kg)	1.45	-
Fibre aspect ratio, l_f/d_f	100, 300 (DS) 100 (TX)	-
$\frac{H_{sample}}{l_f}$	3, 1(DS) 1 (TX)	-
l_f/D_{50}	31, 94 31	-

*DS – Direct Shear ($H_{sample} = 30mm$; $B_{sample} = 60mm$); TX – Triaxial ($H_{sample} = 22mm$; $D_{sample} = 11mm$

*The size in pixels is based on a resolution of 20 μm/px (DS) and 15 μm/px (TX)

4. Sample Preparation

4.1 Direct Shear Test

A first series of tests was carried out with the direct shear box. Square prismatic samples were formed with base and height respectively equal to 60 and 30 mm (as described in ASTM D3080-04). Three sets of samples were prepared, one with natural sand, another with randomly oriented fibres, and one with fibres oriented along 45° angle with respect to the shear plane, i.e., along a direction close to the minimum principal stress.

All samples were prepared compacting sand at an initial void ratio approximately equal to 0.65, corresponding to a relative density Dr=1.0. To identify the most suitable experimental setup, samples were prepared with variable length (lf=10-30mm) and fibre content (χf=0.25-0.50%, computed as fraction by weight of the dry sand), these values chosen in accordance with previous literature studies (Diambra et al., 2010; Lirer et al., 2011; Soriano et al., 2017). Finally, tests with χf=0.50% and lf=30 mm have been chosen as a reference for this study, considering that this length optimises the interlocking with the sand particles (lf/D50≈100) without significantly interacting with the shear box platens.

The samples with randomly oriented fibres were formed mixing sand and fibres, then compacting this

composite material in three subsequent layers within the shear box. Compaction was applied by placing a 3.0 kg weight on the top of each layer and vibrating the material on a table (vibration with 5mm amplitude and 50Hz frequency was applied for a duration of 1'30"). With this procedure fibres tend to assume a sub-horizontal orientation (Soriano et al., 2017). Another set of samples was formed with a specifically conceived procedure to orient fibres at 45° with respect to the shear plane (Fig. 3a). A large block was formed alternatively pouring horizontal layers of pure sand and fibres in a mold (130x60x130mm). The layers approximately 10 mm thick were then compacted on the vibrating table with a weight on the top. The soil mass was then saturated and frozen at a temperature of -10 °C to preserve fabric. The specimens for the shear tests were cut from the frozen sample along ±45°, in order to include the oriented fibres (Fig. 3b).

All shear tests were carried out at a horizontal displacement rate equal to 0.05mm/min.

For each composition, four sister samples were prepared, testing them under the same conditions but interrupting shearing at different horizontal displacements. Finally, one sample represented the initial state before shearing, the other three were representative of the peak, post-peak and ultimate state. This measure was taken to investigate the evolution of the material fabric with tomographic scans. Since this implied to transport samples to the 3SR tomograph, saturation with a mix of nanosilica suspension and sodium chloride solution was applied in the shear box at the end of each test. This material is initially a low viscosity fluid that easily seeps through the soil saturating its pores. Then, due to the reaction between nanosilica and salt solution, it becomes a gel that freezes the soil fabric.

4.2 Miniature Triaxial Test

The response of fibre reinforced sand has also been investigated with triaxial shearing, this time detecting the evolution of material fabric simultaneously performing X-ray tomographic tests. This possibility is given by the combined triaxial and tomographic equipment at Laboratoire 3SR.

To this aim, miniature cylindrical specimens were prepared with diameter and height equal to respectively 11 and 22mm (Fig. 3b, Fig. 3d). Considering the sample diameter, the length of fibres in these tests was fixed to 10 mm. All samples were prepared into a 300μm thick latex membrane, stretched against a rigid mold with vacuum (E. Ando PhD thesis (2013)). The samples with randomly oriented fibres were formed previously mixing sand and fibres, then pouring this composite assembly through a small funnel into the mold forming six layers compacted by vibration up to the desired density. The samples with oriented fibres were formed pouring dry sand in six layers, placing fibres on the top of each stratum in the radial-horizontal direction and applying vibration. All samples were compacted to reach a void ratio on average equal to 0.65 (0.60÷0.68).

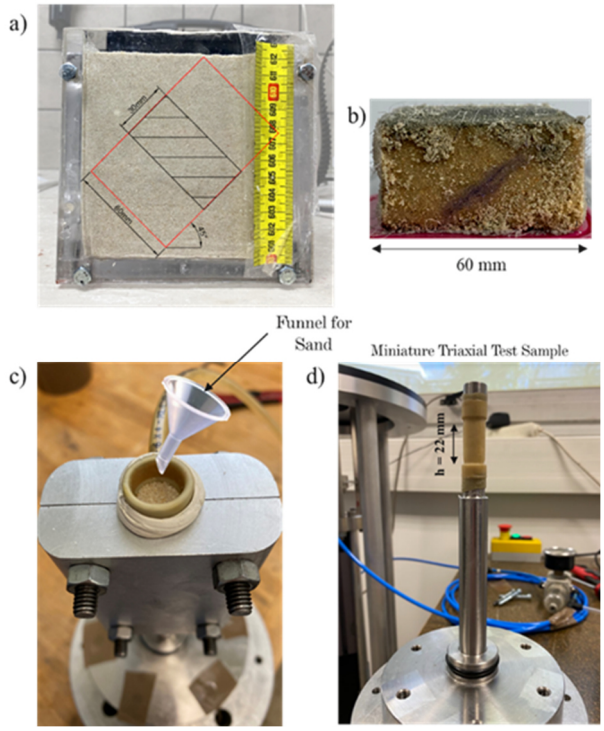

Figure 3. Preparation of a sand sample with oriented fibres for the direct shear tests (a, b) and for the miniature triaxial tests (c, d).

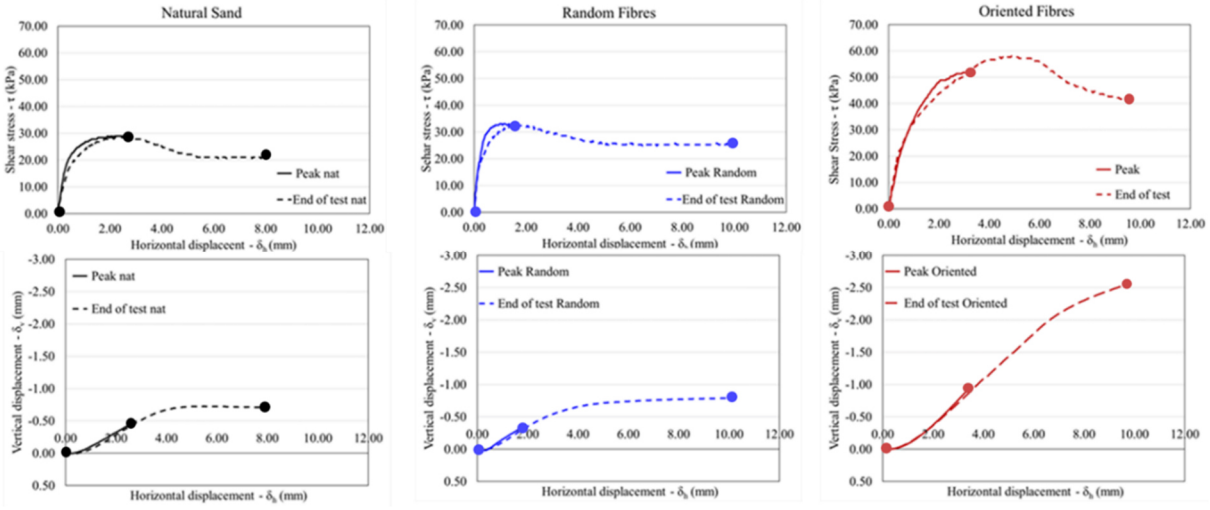

Figure 4. Results of direct shear tests for unreinforced and reinforced samples (vertical effective stress equal to 25 kPa).

5. Element scale response

The response of fibre reinforced sand is firstly analysed phenomenologically, by looking at the stress-displacement curves of direct shear tests, all carried out with 25 kPa vertical effective stress (Fig. 4), and at the stress-strain curves of the miniature triaxial tests, all carried out at 100kPa confining stress (Fig. 5). The tests of Fig. 4, interrupted at different horizontal displacement, show a discrete overlapping, symptomatic of a fair repeatability that enables to attribute the observed differences to the material composition. Both Figs. 4 and 5 show the positive role of fibres reinforcement and, more specifically, of their orientation. Avoiding comments on the initial stiffness, possibly affected by the sample preparation and the compliance of the equipment, both direct and triaxial shear tests show a lower strength for the natural soil, some improvement given by the randomly oriented fibres, and more significant effects when the fibres are oriented along the given direction.

Noteworthy, Fig. 4 shows that the strength enhancement provided by the randomly oriented fibres gives a more fragile response with a peak stress ratio accompanied by dilatancy, followed by a rapid softening and decay of dilatancy. On the contrary, the samples with oriented fibres show a higher strength, (almost double compared with the unreinforced soil), but a different global response. The response is a more ductile, the peak being reached at larger displacements, and dilatancy develops with lower rates compared with the randomly oriented fibres, but for a longer period throughout the test. The volume change is globally higher than for the unreinforced soil and for the randomly oriented fibre reinforcement.

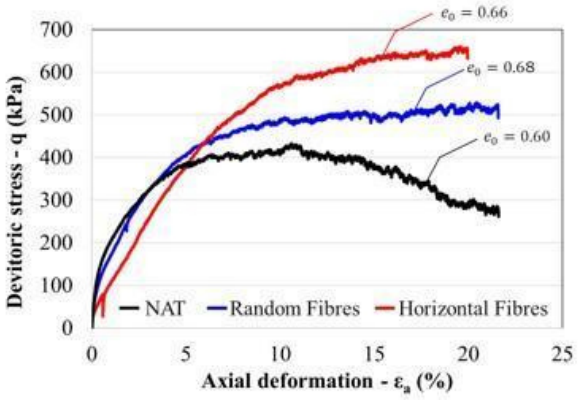

Figure 5. Results of miniature triaxial tests for unreinforced and reinforced samples (effective confining stress equal to 100kPa).

As for the shear strength, a similar trend is observed in the miniature triaxial tests, with the unreinforced soil showing the lowest value, with a substantial increase for randomly oriented fibres and with the largest gain provided by the horizontally oriented fibres (Fig. 5). In these tests, the addition of fibres makes the response more ductile independently on the orientation of fibres. Unfortunately, there is no possibility to quantify dilatancy due to the lack of equipment for measuring volume changes in the miniature triaxial tests. Some comments will be made based on the tomographic images.

6. Microscale analysis

The two sets of tests, direct shear and triaxial, have been accompanied by x-ray tomographies.

One of the aims of this campaign is to understand whether the fibres affect the change in the micro structure and whether it is possible to justify their macroscopically observed effect. The images have been analysed to extract two main quantities: the porosity distribution and the strain fields, through Digital Volume Correlation.

There are currently no direct shear apparatus allowing operando scans that can be tested directly in the tomograph. We therefore tested samples post-mortem in the style of Morgenstern & Tchalenko (1967), who developed the idea of "twin" tests: samples prepared in identical conditions but run and stopped at different stages of the test. The main difficulty is creating sufficiently similar samples and boundary conditions (Fig. 4). The discrete overlapping of curves in Fig. 4 proves the similarity of samples and testing conditions in the present study. The tests were carried out on samples of natural sand, reinforced with a fibre concentration χf=0.50%, and length lf=30mm, and random orientation, as well as with fibres oriented at 45° with respect to the horizontal sliding plane.

For the samples subjected to direct shear, only the porosity maps have been derived. It was not possible to directly measure the local incremental strain fields in the samples through Digital Volume Correlation, given the microstructural difference in the samples.

For the samples subjected to in-operando triaxial tests, maps of maximum axial and volumetric incremental strain have also been computed through Digital Volume Correlation.

Tomographies of a granular specimen contain a huge amount of information on the physical characteristics of the material: grain shape, grain size distribution, porosity field and contact network.

6.1 Direct shear test

From the 3D images at different loading stages of the samples, the porosity fields were computed (calculation step of 10px and calculation volume of 40x40x40px) shown in Fig. 6 using the SPAM software (Stamati et al., 2020).

Fig. 6 shows the porosity fields computed on a vertical plane orthogonal to the shear plane and parallel to the direction of shearing. The porosity variation, determined by dilatancy, is indicative of the shearincerg mechanisms taking place within the sample. The scans are taken at the beginning of tests (initial state), near the peak and at the end of the tests.

The maps show that fibre-packed samples have a more heterogeneous initial porosity field due to the more open structure at the fibre-grain interface. The differences become progressively clearer with sample deformation. At peak and ultimate conditions, volumetric strain in the natural sand sample localises in

a narrow sub-horizontal band, imposed by the equipment, while the fibre-packed samples show a much more diffuse volumetric deformation with higher values at the interface between grains and fibres. This diffusion effect is considerably more pronounced for the sample with fibres oriented at 45°. For this test the increase in porosity takes place in regions parallel to the fibres. The sample with random fibres, on the other hand, shows a response intermediate between the other two cases, showing a clear horizontal shear band as well as the formation of voids related to the local fibre orientation. This difference possibly explains the more brittle or ductile response observed at the element scale (Fig. 4).

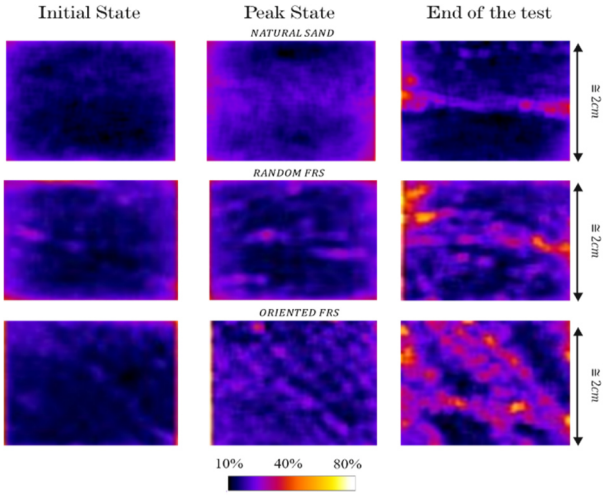

Figure 6. Porosity fields determined by direct shear tests in the initial condition, at peak and ultimate state.

6.2 Triaxial Test

Once the sample is prepared as detailed in section 2.3.2, a 30 kPa vacuum is applied and the sample is placed in the triaxial cell. Then, the sample is isotopically compressed to the desired stress level – 100kPa – by increasing the pressure of the confining fluid and simultaneously releasing the internal vacuum. Once the isotropic phase is completed, the sample is left to rest for 30 minutes; then a shear loading is applied a constant rate of 0.3µm/min. During the tomographies, the displacement is temporarily halted.

6.2.1 Porosity measurements

Considering fibres as voids, Fig. 8 reports the porosity maps for the fibre reinforced and natural samples. For both it is possible to identify a central region where there is an evident variation of porosity especially after 8% of axial strain. The region that changes in porosity tends to take the form of an oblique band, inclined at approximately 45°, indicating a dilatant shear band.

In the case of fibre-reinforced sand samples, a greater volume is involved in the deformation, which suggests that the fibres can mobilise a greater number of grains.

The number of voxels for which porosity changes (and thus the volume of sand belonging to the shear band) is greater in the presence of fibres (Fig. 7). The fibres represent an element of interconnection between the grains. When the grains move in a localised area, a larger number of grains is bound to follow because of this connection.

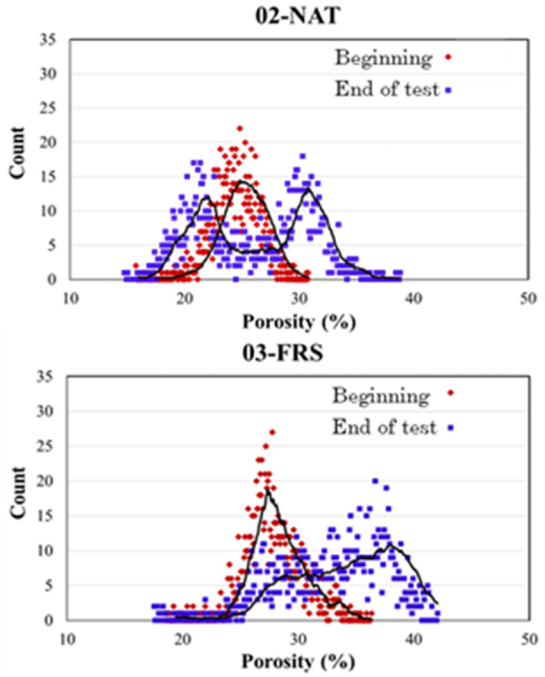

Figure 7. Histograms relating to the comparison of the distribution of porosity within the natural and fibre-reinforced sample, comparing the state of the start and end of the test (0% -20% of axial deformation).

6.2.2 Strain fields

Volumetric and maximum shear strain fields are computed through Digital Volume Correlation using SPAM. In Fig. 8 the incremental field of the first and second invariant of the strain tensor, i.e., the volumetric and maximum shear strain, are reported, for each loading step. As deformation increases, a shear band develops. This indicates that homogeneity is lost from very low strain values and a dilatant shear band develops.

Focusing on the same step of axial strain the localization of deformations is more pronounced in the natural sample. In the fibre-reinforced specimen a bigger amount of volume participates in the shear band.

In the FRS specimen, the width of the shear band increases by approximately 25% corresponding to about 20 grains total size. This confirms the experimental results existing in the literature, as the ones obtained by (Freilich and Zornberg, 2010), in which was observed a significant difference in the failure mode in a drained triaxial test between polypropylene fibre-reinforcement clay specimens and unreinforced samples. Axial deformation of the unreinforced specimen resulted in the development of a failure plane, while the reinforced specimens tended to bulge, indicating an increase in the ductility of the fibre-soil mixture.

In summary, fibre orientation affects the pattern of displacement fields, and fibres hinder localised shear bands, extending them. Fibres can mobilise larger tensile forces, generating diffused strain localisation.

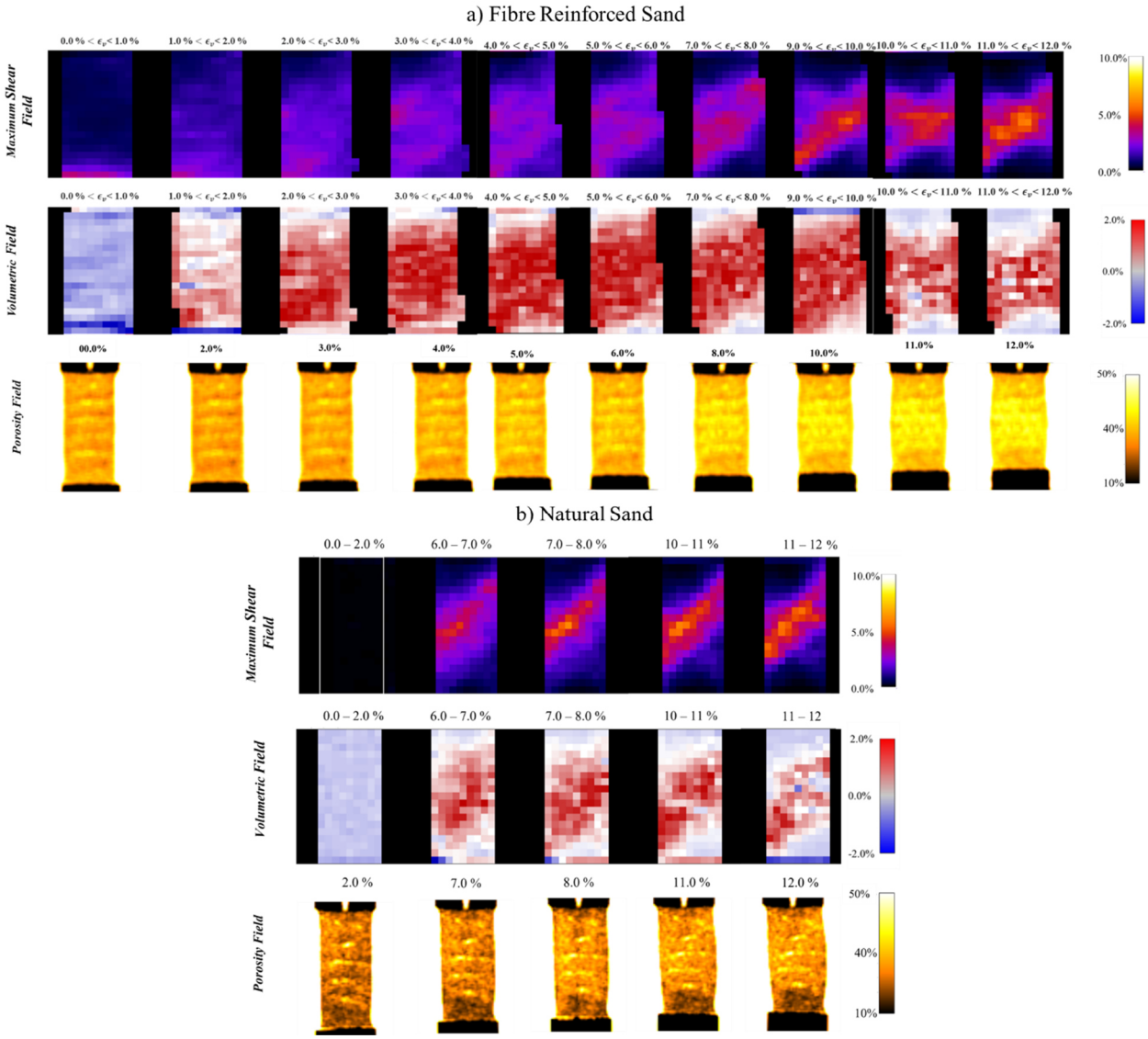

Figure 8. a) Maximum shear strain, volumetric strain and porosity field for fibre reinforced sand sample subjected to triaxial test; b) Maximum shear strain, volumetric strain and porosity field for natural sand sample subjected to triaxial test.

7. Conclusion and perspectives

If adequately activated, fibres tension modifies the strain pattern of the samples, preventing the fragile rupture along a shear band, transferring stresses to the outer soil portions, in this way providing a more dilatant and ductile overall response of the reinforced material.

Length and fibre content influence the mechanical behaviour of sands (greater dilatancy - higher peak strength - higher ductility), confirming results from the literature.

Fibre orientation plays a key role; fibres must undergo tensile stress to produce enhancement, therefore, they must be oriented to ensure maximum interaction with the shear bands. The presence of fibres affects the porosity field in each condition, in the presence or absence of strain, as the fabric of the specimen is modified.

The strain is more homogeneous and diffuse in the presence of fibres and the shear band thickness is larger.

The fibres can resist extension stress, hence, it could be very interesting to perform triaxial tensile tests, to quantify the tensile strength contribution conferred to the soil. The fibres improve the mechanical properties of the sands during compression, if they were also able to transfer a sufficient amount of tensile strength to the soil, the fibre reinforcement technique would be of considerable interest in engineering applications.

References

Ahmad, F., Bateni, F., & Azmi, M. 2010. "Performance evaluation of silty sand reinforced with fibres", In: Geotextiles and geomembranes, 28(1), 93-99. https://doi.org/10.1016/j.geotexmem.2009.09.017

Alikarami, R., Andò, E., Gkiousas-Kapnisis, M. et al. "Strain localisation and grain breakage in sand under shearing at high mean stress: insights from in situ X-ray tomography ", In: Acta Geotech. 10, 15–30 2015. https://doi.org/10.1007/s11440-014-0364-6

Alshibli, K. A., & Alramahi, B. A. (2006). "Microscopic evaluation of strain distribution in granular materials during shear", In: Journal of geotechnical and geoenvironmental engineering, 132(1), 80-91. https://doi.org/10.1061/(ASCE)1090-0241(2006)132:1(80)

Al-Refeai, T. O. (1991). "Behavior of granular soils reinforced with discrete randomly oriented inclusions", In: Geotextiles and Geomembranes, 10(4), 319-333. https://doi.org/10.1016/0266-1144(91)90009-L

Andò, E., Viggiani, G., Desrues, J. 2020. "X-Ray Tomography Experiments on Sand at Different Scales", In: Giovine, P., Mariano, P.M., Mortara, G. (eds) Views on Microstructures in Granular Materials. Advances in Mechanics and Mathematics (), vol 44. Birkhäuser, Cham. https://doi.org/10.1007/978-3-030-49267-0_1

Consoli, N. C., Vendruscolo, M. A., Fonini, A., & Dalla Rosa, F. 2009. "Fiber reinforcement effects on sand considering a wide cementation range", In: Geotextiles and Geomembranes, 27(3), 196-203. https://doi.org/10.1016/j.geotexmem.2008.11.005

Consoli, N. C., Heineck, K. S., Casagrande, M. D. T., & Coop, M. R. 2007. "Shear strength behavior of fiber-reinforced sand considering triaxial tests under distinct stress paths", In: Journal of geotechnical and geoenvironmental engineering, 133(11), 1466-1469.

Diambra, A., & Ibraim, E. 2015. "Fibre-reinforced sand: interaction at the fibre and grain scale", In: Géotechnique, 65(4), 296-308. https://doi.org/10.1680/geot.14.P.206

Diambra, A., Ibraim, E., Wood, D. M., & Russell, A. R. 2010. "Fibre reinforced sands: experiments and modelling", In: Geotextiles and geomembranes, 28(3), 238-250. https://doi.org/10.1016/j.geotexmem.2009.09.010

Edward Ando. "Experimental investigation of microstructural changes in deforming granular media using x-ray tomography", In: Mechanics [physics.med-ph]. Université de Grenoble, 2013. English. ⟨NNT: 2013GRENI097⟩. ⟨tel-01144326⟩.

Freilich, B. J., Li, C., & Zornberg, J. G. 2010. "Effective shear strength of fiber-reinforced clays", In 9th international conference on geosynthetics, Brazil (pp. 1997-2000).

Gao, Z., Lu, D., & Huang, M. 2020. "Effective skeleton stress and void ratio for constitutive modeling of fiber-reinforced sand", Acta Geotechnica, 15(10), 2797-2811. https://doi.org/10.1007/s11440-020-00986-w

Gray, D. H., & Ohashi, H. 1983. "Mechanics of fiber reinforcement in sand", Journal of geotechnical engineering, 109(3), 335-353. https://doi.org/10.1061/(ASCE)0733-9410(1983)109:3(335)

Gong, L., Nie, L., Liu, C. et al. "Modelling Triaxial Tests on Fibre-Reinforced Sands with Different Fibre Orientations Using the Discrete Element Method", In: KSCE J Civ Eng 24, 2268–2280 2020. https://doi.org/10.1007/s12205-020-1050-x

Ibraim, E., Diambra, A., Russell, A. R., & Wood, D. M. 2012. "Assessment of laboratory sample preparation for fibre reinforced sands", In: Geotextiles and Geomembranes, 34, 69-79. https://doi.org/10.1016/j.geotexmem.2012.03.002

Lirer, S., Flora, A., & Consoli, N. C. 2011. "On the strength of fibre-reinforced soils", In: Soils and foundations, 51(4), 601-609. https://doi.org/10.3208/sandf.51.601

Maher, M. H., & Ho, Y. C. 1994. "Mechanical properties of kaolinite/fiber soil composite", In: Journal of Geotechnical Engineering, 120(8), 1381-1393. https://doi.org/10.1061/(ASCE)0733-9410(1994)120:8(1381)

Matsushima, T., Uesugi, K., Nakano, T., & Tsuchiyama, A. 2006. "Visualization of Grain Motion inside a Triaxial Specimen by Micro X-ray CT at SPring-8", In: Advances in X-ray Tomography for Geomaterials, 255-261. https://doi.org/10.1002/9780470612187.ch24

Michalowski, R. L., & Cermak, J. 2002. "Strength anisotropy of fiber-reinforced sand", In: Computers and Geotechnics, 29(4), 279-299. https://doi.org/10.1016/S0266-352X(01)00032-5

Park, T., & Tan, S. A. 2005. "Enhanced performance of reinforced soil walls by the inclusion of short fiber", In: Geotextiles and geomembranes, 23(4), 348-361. https://doi.org/10.1016/j.geotexmem.2004.12.002

Salvatore, E., et al. "Geostatistical analysis of strain localization in triaxial tests on sand." In: Géotechnique Letters 9.4 (2019): 334-339. https://doi.org/10.1680/jgele.18.00228

Soriano, I., Ibraim, E., Ando, E., Diambra, A., Laurencin, T., Moro, P., & Viggiani, G. 2017. "3D fibre architecture of fibre-reinforced sand", In: Granular Matter, 19(4), 1-14. https://doi.org/10.1007/s10035-017-0760-3

Stamati, O., Andò, E., Roubin, E., Cailletaud, R., Wiebicke, M., Pinzon, G., ... & Birmpilis, G. 2020. "Spam: software for practical analysis of materials", In: Journal of Open Source Software, 5(51), 2286. https://doi.org/10.21105/joss.02286

Tang, C., Shi, B., Gao, W., Chen, F., & Cai, Y. 2007. "Strength and mechanical behavior of short polypropylene fiber reinforced and cement stabilized clayey soil", In: Geotextiles and Geomembranes, 25(3), 194-202. https://doi.org/10.1016/j.geotexmem.2006.11.002

Yetimoglu, T., Inanir, M., & Inanir, O. E. 2005. "A study on bearing capacity of randomly distributed fiber-reinforced sand fills overlying soft clay", In: Geotextiles and Geomembranes, 23(2),174-83. https://doi.org/10.1016/j.geotexmem.2004.09.004